

## Supplementary File

**Construction strategy of flexible and breathable SiO<sub>2</sub>/Al/NFs/PET composite fabrics with dual shielding against microwave and infrared-thermal radiations for wearable protective clothing**

Hui Ye <sup>1,2</sup>, Qiongzhen Liu <sup>1,2\*</sup>, Xiao Xu <sup>1,2</sup>, MengYa Song <sup>1,2</sup>, Ying Lu <sup>1,2</sup>, Liyan Yang <sup>1,2</sup>, Wen Wang <sup>1,2</sup>, Yuedan Wang <sup>1,2</sup>, Mufang Li <sup>1,2</sup>, Dong Wang <sup>1,2\*</sup>

<sup>1</sup> Key Laboratory of Textile Fiber and Products, Ministry of Education, Wuhan Textile University, Wuhan 430200, China

<sup>2</sup> Hubei International Science and Technology Cooperation Base for Intelligent Textile Material Innovation & Application, Wuhan Textile University, Wuhan 430200, China

**\*Corresponding Author:** Qiongzhen Liu, windlqz\_2000@163.com; Wang Dong, wangdon08@126.com

**List of Figures:**

**Figure S1. Changes in thickness and surface roughness for (a-b) Al films and (c-d) SiO<sub>2</sub> films sputtered on a glass substrate with respect to sputtering time.**

**Figure S2. Influence of the relative humidity on the electromagnetic shielding effectiveness of the S4-1 fabric: (a) SE<sub>T</sub>, (b) SE<sub>R</sub>, and (c) SE<sub>A</sub>.**

**Table S1. IR temperature variations between the test fabric specimens and the hot plate center.**

**Figure S3. UV-Vis-NIR spectra of the various SiO<sub>2</sub>/Al/NFs/PET fabrics with different surface arrays: (a) reflectivity, and (b) transmissivity.**

**Movie S1. A movie showing water vapor in a closed container penetrating through a SiO<sub>2</sub>/Al/NFs/PET fabric, proving the breathability of the fabric.**

**Figure S4. The SiO<sub>2</sub>/Al/NFs/PET conductive fabric (S4-1) showing asymmetric surface wetting properties toward water with (a) hydrophilic PET side and (b) hydrophobic coating side.**

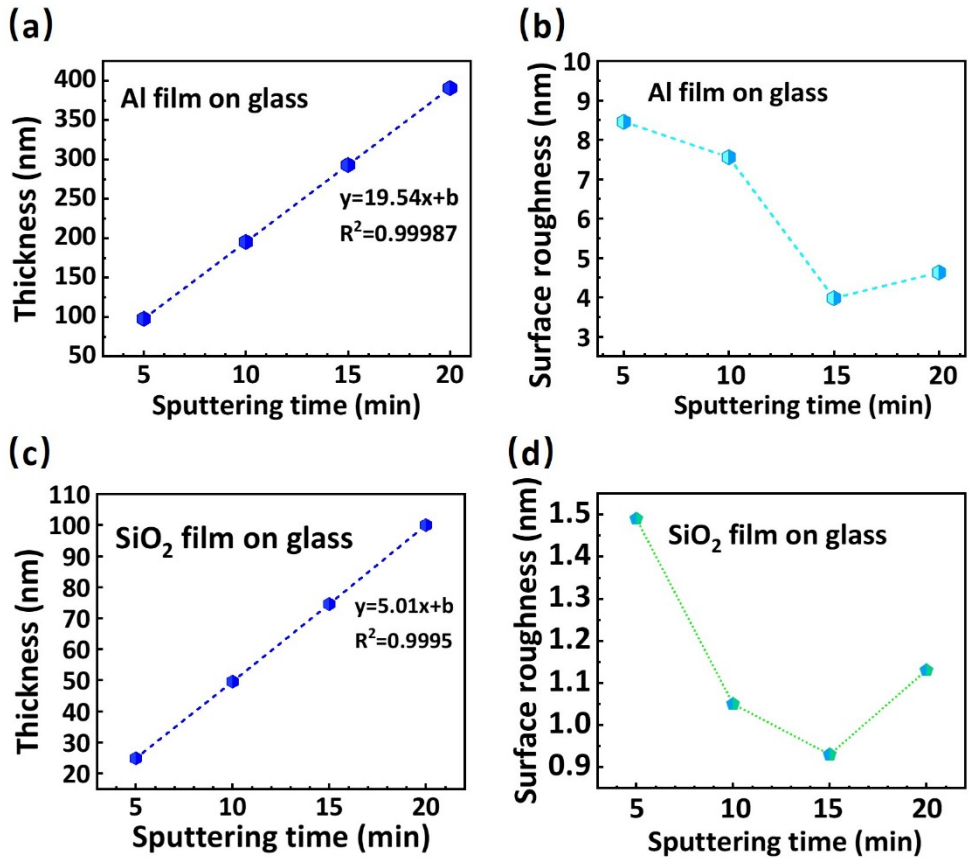
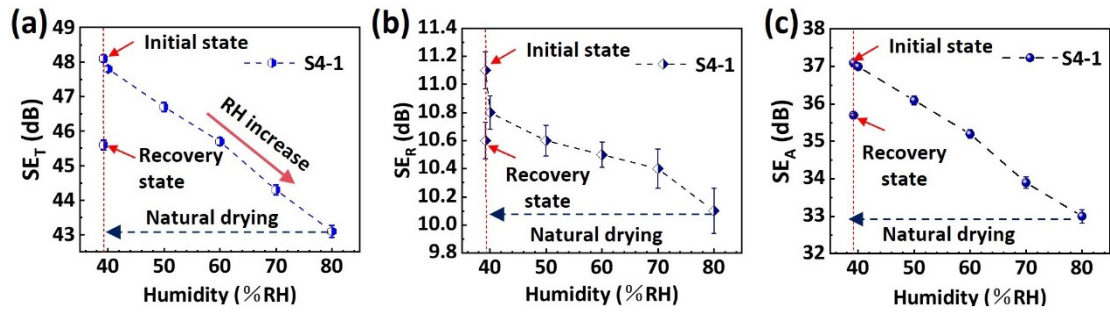


Figure S1. Changes in thickness and surface roughness for (a-b) Al films and (c-d) SiO<sub>2</sub> films sputtered on a glass substrate with respect to sputtering time.



**Figure S2. Influence of the relative humidity on the electromagnetic shielding effectiveness of the S4-1 fabric: (a)  $SE_T$ , (b)  $SE_R$ , and (c)  $SE_A$ .**

**Table S1. IR temperature variations between the test fabric specimens and the hot plate center.**

<b>Fabric samples</b>	<b>IR temperature of samples (°C)</b>	<b>Hot stage temperature (°C)</b>	<b><math>\Delta T</math> (°C)</b>
S4	20.4		-24.6
S4-1	20.1		-24.9
S4-1-1	19.6		-25.4
S4-1-1.5	19.2	45	-25.8
S4-1-6	18.8		-26.2
S4-1-7.5	18.4		-26.6
S4-1-9	18.4		-26.6

**Note:**  $\Delta T$  denotes the IR temperature variation between the test fabric specimen and the hot plate center

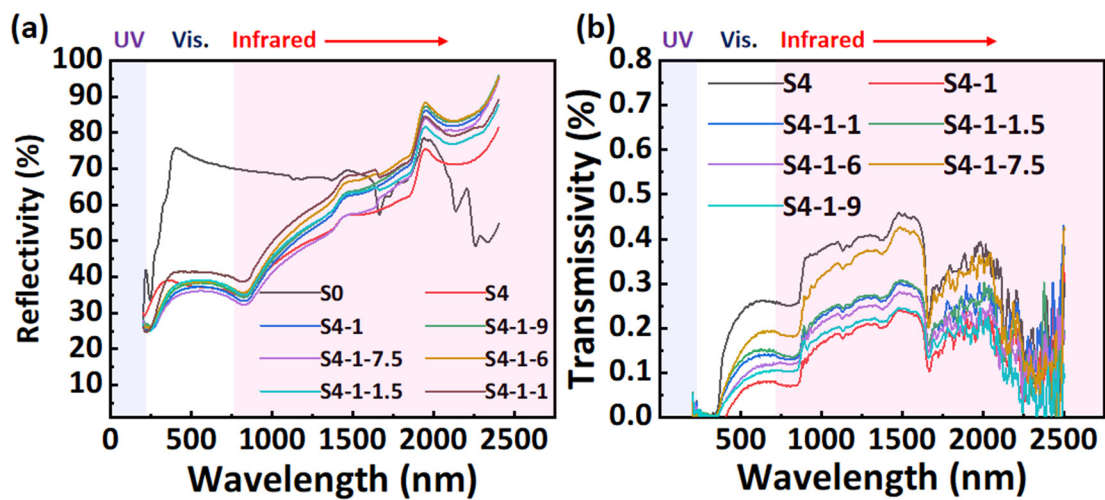
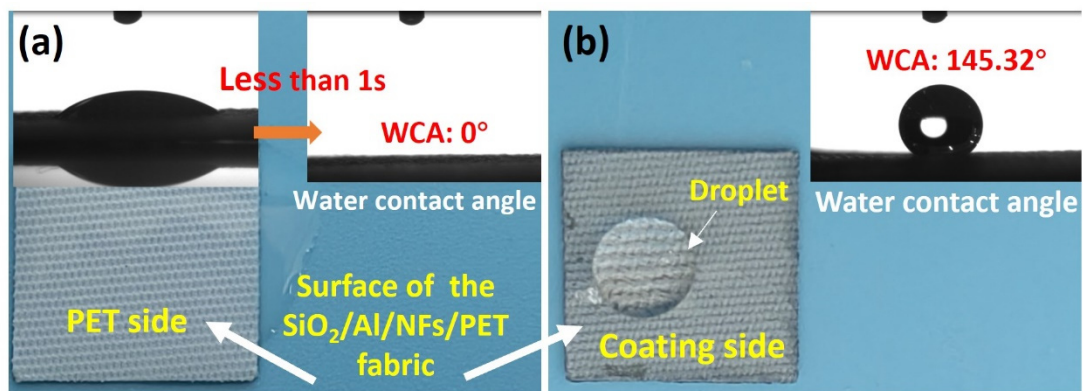


Figure S3. UV-Vis-NIR spectra of the various  $\text{SiO}_2/\text{Al}/\text{NFs}/\text{PET}$  fabrics with different surface arrays: (a) reflectivity, and (b) transmissivity.

**Movie S1. A movie showing water vapor in a closed container penetrating through a SiO<sub>2</sub>/Al/NFs/PET fabric, proving the breathability of the fabric.**



**Figure S4.** The  $\text{SiO}_2/\text{Al}/\text{NFs}/\text{PET}$  conductive fabric (S4-1) showing asymmetric surface wetting properties toward water with (a) hydrophilic PET side and (b) hydrophobic coating side.